Establishment of a Murine Model of Acute-on-Chronic Liver Failure with Multi-organ Dysfunction

Nidhi Nautiyal
Institute of Liver and Biliary Sciences
Deepanshu Maheshwari
Institute of Liver and Biliary Sciences
Dhananjay Kumar
Institute of Liver and Biliary Sciences
Rekha Kumari
Institute of Liver and Biliary Sciences
Suchi Gupta
All India Institute of Medical Sciences
Sachin Sharma
Amity University
Sujata Mohanty
All India Institute of Medical Sciences
Anupama Parasar
Institute of Liver and Biliary Sciences
Chhagan Bihari
Institute of Liver and Biliary Sciences
Subhrajit Biswas
Amity University
Archana Rastogi
Institute of Liver and Biliary Sciences
Rakhi Maiwall
Institute of Liver and Biliary Sciences
Anupam Kumar
Institute of Liver and Biliary Sciences
Shiv Kumar Sarin (shivsarin@gmail.com)
Institute of Liver and biliary Sciences https://orcid.org/0000-0002-0544-5610

Research Article

Keywords: Liver failure, animal models of liver disease, Acute Kidney Injury (AKI), Ascites, Lipopolysaccharide, portal hypertension, ACLF

Posted Date: April 26th, 2021

DOI: https://doi.org/10.21203/rs.3.rs-438031/v1

Version of Record: A version of this preprint was published at Hepatology International on August 25th, 2021. See the published version at https://doi.org/10.1007/s12072-021-10244-0.

Abstract

Background and Aims: Acute-on-chronic liver failure (ACLF) is a distinct clinical entity with high probability of organ failure and mortality. Experimental models of ACLF are needed to understand the pathophysiology and natural course of the disease.

Methodology and Results: To mimic the syndrome of ACLF, chronic liver disease was induced by intra-peritoneal administration of carbon tetrachloride (CCl_4) for 10 weeks, followed by acute injury with acetaminophen (APAP) and lipopolysaccharide (LPS) administration. Blood, ascitic fluid and organs were collected to study cell death, regeneration and fibrosis. APAP/LPS induced second insult to the CCL_4 animals showed progressive and significant increase in bilirubin ($p < 0.05$), prothrombin time ($P < 0.0001$) and blood ammonia ($p < 0.001$) post-acute injury similar to human ACLF. Ascites was noticed by day 11 (median serum-ascites albumin gradient, SAAG ((1.2(1.1–1.3) g/dL) suggestive of portal hypertension. At 24 hours post-APAP/LPS infusion, the liver tissue showed increased hepatocyte ballooning and endothelial cell TUNEL positivity. This was followed by progressive hepatocyte necrosis from perivascular region at day 7 to lobular region by day 11 acute injury. They also showed regression in fibrous septa ($p < 0.005$) in comparison to cirrhosis. A progressive loss of hepatic regeneration (proliferating cell nuclear antigen; $p < 0.005$) was also seen following APAP/LPS injury. These animals also showed a significant increase in serum creatinine ($p < 0.05$) levels and renal tubular injury by day 11 which was not present in cirrhotic animals.

Conclusion: The CCL4/APAP/LPS (CALPS) model of ACLF mimics the clinical, biochemical and histological features of ACLF with demonstrable progressive hepatocyte necrosis, liver failure, impaired regeneration, development of portal hypertension and organ dysfunction in an animal with chronic liver disease.

Introduction

Acute-on-chronic liver failure (ACLF) is an increasingly recognized clinical entity encompassing an acute liver failure in patients with underlying chronic liver disease or cirrhosis, resulting in cascade of event leading to sepsis, multi-organ failure (MOF) and death [(1–6)]. Clinical management is still challenging due to limited treatment options. Liver transplantation is the only curative treatment for such patients, which is however feasible in a small proportion of patients with ACLF [(7)].

One of the major challenges in the ACLF is the poor understanding of underlying pathophysiology leading to rapid progression of liver injury, sepsis and MOF. There is also a need to understand the dynamic course of hepatic injury with alterations in immune mediators and development of immunoparesis in this disease state. Hence, a representative experimental model that mimics the course of human ACLF is

crucial to decipher the pathophysiological journey of the disease and development of new therapeutic strategies for improved clinical outcomes for ACLF patients.

Several experimental models of ACLF have been reported [8–12] but none of them reproduces the clinical and pathological process of ACLF. In most models of ACLF, the chronic injury has been induced by carbon tetrachloride (CCl_4), bile duct ligation or porcine serum whereas the acute injury was induced by D-galactosamine/lipopolysaccharide (LPS) [8–12]. Though, these models showed histological features for the presence of both chronic and acute liver injury, the mean survival period was very short after the acute insult and rarely showed development of portal hypertension, ascites and MOF; a common feature of human ACLF. Recently, Xiang et al [13] have developed a mouse model of sepsis induced ACLF that provide the survival window to understand the pathophysiology of liver failure in response to infection and liver injury. However, this model did not define whether the secondary organ failure is because of bacteremia or liver failure. and does not address hepatic regeneration. Sepsis is a precipitant or consequence of ACLF is still debatable [14–16]. According to the APASL criteria [17–18] sepsis is a complication which follows on-going hepatocellular necrosis and occurs due to liver failure induced immune paresis [1, 19, 20]. To carefully evaluate the sequence of events, there is a need of an ACLF model which can reproduce this spectrum of human ACLF progression to understand the advancement of liver failure and its impact on organ dysfunction and immune injury.

Acute hepatic insult in ACLF has been thought to occur due to inappropriate and widespread activation of the inflammatory cytokine pathway; release of damage-associated proteins and other cytokines from dying parenchymal and non-parenchymal cells, intestinal endotoxemia as a result of increased bacterial translocation/bacterial products from the gut into the portal circulation [1, 21–22]. In the current study, we developed a mouse model of ACLF by chronic administration of CCl_4 to produce chronic liver injury/cirrhosis followed by an acute insult with acetaminophen (APAP) and a low dose of lipopolysaccharide (LPS); the CALPS model, to mimic the situation of an acute insult on a chronic liver disease along with introduction of intestinal endotoxemia. The present model was developed with an aim to investigate whether the progression of liver injury to liver failure in animals with pre-existing chronic liver disease/cirrhosis leads to subsequent development of portal hypertension, sepsis, and secondary organ dysfunction. The concomitant processes of hepatic regeneration, and injury to other organs was carefully studied in the presence of on-going liver failure. The sole aim was to see whether the sequence of animal experiments and the resulting murine disease model, resembles the syndrome of ACLF seen in human beings.

Methods

Animals

Six-to-eight week old male C57Bl6 mice were purchased from LIVEON BioLabs Pvt. Ltd, Karnataka, India. Animals were housed in the Institutional Animal Facility in a clean, temperature controlled environment

with a 12hrs light and dark cycle and were provided with free access to regular laboratory chow diet and water. Animal care and all experimental procedures were approved by the Institutional Animal Ethics Committee (IAEC) under the project approval (IAEC/ILB/17/03) from Department of Science and Technology, Government of India.

Study Design

All animals were randomly divided into two groups (control: n = 10; treatment group: n = 45). The treatment group received a mixture of carbon-tetrachloride (CCl_4; Central Drug House, Delhi, India) in Olive oil (HiMedia Pvt. Ltd., India) intraperitoneally (i.p) at a dose of 0.1ml/kg to 0.5ml/kg twice per week for ten weeks to generate chronic liver injury model. After ten weeks, mice (n = 5) were euthanized to confirm the grade of cirrhosis. Mice for ACLF model were further divided based on the dose administration, LPS and Acetaminophen (APAP) in different groups; Group 1: LPS (Sigma, 100µg/kg, n = 6); Group 2 (APAP,), 600mg/kg, n = 6); Group 3 (LPS (50µg/kg) + APAP (350mg/kg), n = 28)). Mice were fasted for 12hrs before the dose of APAP. APAP was dissolved in saline (0.9% V/V) and warmed to ambient body temperature before i.p. injection. Sixty minutes later, these mice were given i.p. injection of LPS. All animals were given humane care in compliance with the IAEC guidelines and monitored for different time interval i.e. 24hr, Day 7 and Day 11. The data was collected on the basis of changes in blood biochemical parameters and histology. Detailed methodology of sample collection, histo-pathological and biochemical analysis are mentioned in supplementary data sheet.

Results

Induction of ACLF in mice by the combination of chronic and acute liver injury and low-grade endotoxemia

Development of Chronic Liver Disease:

To induce chronic liver injury, C57Bl6 male mice (6–8 weeks) were subjected to intraperitoneal injection of successive doses of CCL_4 for 10 weeks (twice a week). After 10 weeks of chronic CCL_4 administration biochemical analysis of blood plasma showed a significant increase in ALT ($p < 0.0001$), AST ($p < 0.0001$), total bilirubin ($p < 0.001$) and decrease in albumin ($p < 0.0001$) but they did not show any feature of hepatic decompensation like ascites or increase in the level of blood ammonia (figure S1A).

In comparison to healthy, post-CCl_4 injury, liver tissue showed enhanced portal inflammation (with the collection of immature calls, blasts, plasma cells and few PMNs) with thin grade II to III bridging fibrosis and necrosis. Hepatocytes showed eosinophilic cytoplasm with enlarged reactive nucleus (figure S1B). Altogether, these data confirmed the presence of chronic liver disease/cirrhosis after 10 weeks of chronic CCl_4 administration in mice. Further analysis of plasma creatinine and blood urea nitrogen (figure S2A) were comparable to healthy mice after CCl_4 injury and they did not show any injury to kidney (figure S2B) and lung (figure S2C); suggesting no secondary organ dysfunction or injury.

Induction of Acute Injury:

To induce ACLF in chronic liver injured/cirrhosis mice, we initially used three different combinations of acute liver injury. After 10 weeks of CCl_4 injury, animals were divided into 3 groups (n = 6, each group). Group 1 received high dose of LPS (100ug/kg), group-2 received high dose of APAP (600mg/kg) and group-3 received low dose of APAP (350mg/Kg) + Low dose of LPS (50ug/kg). While all the animals in group 1 and 2 died within 48 hours of acute injury, the animals in group 3 did not show any short-term mortality and developed features of human ACLF. These animals showed presence of ascites, liver necrosis, inflammation and acute tubular necrosis (figure S3A & B). Hence, we used this combination further for the development of ACLF and analysis of pathophysiological changes in the progression of ACLF model.

As described in Fig. 1a, after 10 weeks of CCl_4 injury, ACLF (n = 22) was induced by the combination of APAP and LPS and animals were sacrificed at 24hrs (n = 5, day 7(n = 5) and d11 (n = 10) post LPS treatment. Two animals died between days 3–5. Post-APAP and LPS injury while there was no significant change in plasma AST and albumin (except an increase in AST ($p < 0.05$) at day 11 in comparison to cirrhosis, there was a progressive increase in plasma ALT ($p < 0.001$), prothrombin time ($p < 0.001$), bilirubin ($p < 0.01$) and blood ammonia ($p < 0.001$) (Fig. 1b) suggesting progressive liver failure. The animals showed the presence of ascites and jaundice at day 11 and were sacrificed then (Fig. 1C). Further analysis of ascitic fluid showed a serum-ascites albumin gradient (SAAG) of > 1.1g/dl (Fig. 1D) indicating that the ascites is due to portal hypertension.

Altogether, the animals showed characteristic clinical and biochemical features of human ACLF as an increase in bilirubin (jaundice), prothrombin time (coagulopathy), blood ammonia and occurrence of ascites.

APAP with LPS induces progressive liver injury and inflammation

Histological analysis of liver tissue at 24hrs, day 7 and day 11 post-APAP and LPS treatment showed persistent portal inflammation (Fig. 2A). In comparison to cirrhosis liver, 24 hour post-APAP and LPS treatment, the hepatocytes showed a marked change in their morphology in terms of ballooning and peripheral condensation of organelles with rigid appearance of the cell membrane (Fig. 2A, S4A), which reduced till day 11. However, there was an increase in necrosis from day 7 to day 11 (Fig. 2A) and presence of cholestasis at day 11 (figure S4B), this is quite characteristic in human ACLF as well. To confirm liver injury TUNEL assay were performed. In cirrhosis livers, the TUNEL positivity was mainly confined to immune cells near the fibrotic septa. However, at 24 hour post-injury, the presence of apoptosis was seen around the vascular regions having most of the endothelial and liver infiltrating cells. This was seen to increase at day 7 with the hepatocyte death surrounding the vascular niche. However, at day 11, the hepatocyte death further progressed to the lobular areas and showed marked differences at the level of apoptosis early (peri-nuclear TUNEL+) as well as late-stage (Nuclear TUNEL+) (Fig. 2B, S4C).

In further western blot analysis while faint band of cleaved caspage-3 were observed at 24 hour post-acute injury there was no Cleaved caspage-3 expression at day − 11 (Fig. 2C), this suggest that hepatocyte death in this model is mainly because of necrosis. Similarly, the Ly6g positivity enhanced from 24Hrs to day 11 (figure S4D) suggesting activation of neutrophils at day 11 of post-acute injury.

To investigate the changes in inflammatory responses, we analyzed the expression of pro- (IL-6, IL-1β, TNF-α) and anti- (IL10) inflammatory cytokines in liver tissue by q-RTPCR and infiltration of Ly6G + neutrophil by immunohistochemistry. In comparison to cirrhosis animals, while there was a persistent increase in pro-inflammatory cytokines namely IL6, TNF-α and IL-1β starting from 24 hours (Fig. 2D); the expression of anti-inflammatory cytokines (IL10) (Fig. 2E) showed increase by day 7 post-APAP and LPS treatment. Similarly, the number of Ly6G + neutrophil significantly increased from 24Hre to day-11 (figure S4D). Altogether, these data show the presence of progressive liver injury, neutrophil infiltration and cytokine storm similar to what is witnessed in human ACLF. With APAP and LPS treatment, liver injury begins with hepatocyte ballooning, vascular injury and portal inflammation leading to and perpetuating hepatocyte death.

APAP with LPS treatment causes regression of liver fibrosis in cirrhosis

APAP and LPS treatment induced a significant reduction in fibrosis measured by MT and Sirius red. In comparison to chronic liver injury/cirrhosis liver, in the post-APAP and LPS treated animals there was reduction in the level of fibrosis from 24 hours of treatment till day 11. MT staining showed the reduction from 41.2%±2.1 ($p < 0.0001$) at 24h to 22.9%±2.1 ($p < 0.0001$) at day 7, and 13.1%±1.2 ($p < 0.0001$) at day 11. Similarly, Sirius red staining reduced to 82.2%±2.4 ($p < 0.01$) at 24h, 50.6%±1.6 ($p < 0.0001$) at day 7, and 16.7%±1.6 ($p < 0.0001$) at day 11 (Fig. 3A). To validate the reduction in fibrosis, we did collagen I staining and found it to be reduced from 85.2%±4.1 ($p = 0.02$) at 24h; 40.3%±1.3 ($p < 0.0001$) on day 7 and 33.3%± 3.9 ($p < 0.0001$) on day 11 (Fig. 3B). A reduction in the number of α-SMA + myofibroblasts through apoptosis is a key early event during fibrosis resolution. The amount of α-SMA staining post-APAP and LPS treatment significantly reduced to 81.2%±1.4, $p = 0.01$at day 7 and 58.6%±2.4, $p < 0.0001$ at day 11 of cirrhosis (Fig. 3C). Hence, the reduction of α-SMA + myofibroblasts in response to APAP and LPS induced acute injury might seems to have contributed in the regression of fibrosis in this animal model.

ACLF induces regeneration failure in cirrhosis

Acute injury triggers hepatic regeneration [(23)], however, we observed progressive symptoms of liver failure in terms of increase in bilirubin, prothrombin time, and blood ammonia post-APAP and LPS injury in CCL_4 models of chronic liver disease (Fig. 1B). Hence, we checked the effects of APAP and LPS induced liver injury on hepatic regeneration by analyzing the proliferating cell nuclear antigen (PCNA) positive hepatocyte for hepatocyte proliferation and CK-19 positive ductular cells for hepatic progenitor cell-mediated liver regeneration. At cirrhosis level there were 66 ± 1.5 PCNA + hepatocytes per high power field which were significantly reduced from 24 hours to day 11 (46 ± 2.7 by 24 hours ($P < 0.001$); 10 ± 3.2 by

day 7 ($p < 0.0001$) and 3 ± 1.2 by day 11 ($p < 0.0001$)) post-acute injury (Fig. 4a & b). This suggests a progressive loss of hepatocyte proliferation after post-APAP and LPS induced acute injury. Similar to hepatocyte proliferation, the number of CK-19 + ductular cells also reduced in the cirrhotic animals at 24 hour and day 7 with slight increase at day 11 from day 7 (Fig. 4C & D). Our animal model did not show significant ductular reaction, an indicator of progenitor cell-mediated liver regeneration.

APAP with LPS induced liver injury induces systemic organ dysfunctions

Systemic organ dysfunctions are the common features of ACLF in human [1]. ACLF patients are more susceptible to renal dysfunction which is associated with severe outcome. To check extra-hepatic manifestation of ACLF, we analyzed the levels of serum creatinine and blood urea nitrogen (BUN). While there was no significant change in the level of creatinine by day 7 post-APAP and LPS, it was significantly ($p < 0.01$) increased at day 11. Similarly, the level of BUN also increased significantly ($p < 0.05$) at Day 11 (Fig. 5A) suggesting renal dysfunction. Further, the analysis of kidney histology showed marked presence of acute tubular necrosis (ATN) at day 11 ($n = 8$; 80%), suggesting renal dysfunction in response to APAP/LPS induced ACLF is due to structural damage of kidney (Fig. 5B).

The histology of lungs showed no changes at week 10 of chronic liver injury, 24hrs and day 7. There was presence of pulmonary dysfunction (interstitial pneumonia and exudate pneumonia) at day 11 in 3 of 10 (30%) mice samples (figure S5).

Altogether, these data suggest that liver failure induces systemic organ dysfunctions in this animal model of ACLF.

Discussion

The underlying cause of rapid and progressive liver failure leading to sepsis, MOF and high mortality in ACLF is poorly defined [17–18, 25]. Hence, there is need for representative experimental model that mimics the course of human ACLF to decipher the pathophysiological journey of the disease and development of new therapeutic strategies. In the current study, we developed a mouse model of progressive ACLF, the CALPS model that resembles the clinical and histological features of human ACLF [17, 18]. This model demonstrates that acute liver injury with endotoxemia in cirrhosis leads to progressive hepatocyte necrosis without liver regeneration leading to liver failure and development of secondary organ injury. This model helped to investigate the hypothesis that perpetual presence of hepatotoxin and intestinal endotoxemia lead to hepatocellular necrosis along with inappropriate and widespread activation of the inflammatory cytokine pathway leading to liver failure and subsequent secondary organ failure/sepsis in ACLF [1, 19, 21–22].

Several approaches have been reported in the past by various groups to develop the ACLF model using D-galactosamine/lipopolysaccharide (LPS) [8–12]. Though these models showed histological features for the presence of both chronic and acute liver injury, they failed to recapitulate the whole pathological

process of this disease due to high short-term mortality and lack the presence of ascites, encephalopathy and secondary organ dysfunction; common features of human ACLF. It is also difficult to understand in these models, whether the high short-term mortality is due to liver failure or endotoxin induced shock.

We showed that modest doses of APAP and LPS are sufficient to trigger the liver injury followed by hepatic decompensation (as evident by the presence of jaundice, coagulopathy, ascites and rise in blood ammonia in the current model) and secondary organ injury similar to human ACLF. Our data shows that in response to APAP/LPS injury in cirrhosis liver, there is marked increase in hepatocyte ballooning and endothelial/ immune cell death within 24 hours followed by progressive increase in hepatocyte necrosis from day 7 to 11. This leads to cytokine storm with a persistent increase in pro-inflammatory cytokines (IL6, TNFα and IL-1β) starting from 24 hours and followed by an increase in expression of anti-inflammatory cytokines (IL10) by day 7 post-acute injury with increase neutrophil infiltration. Manifestation of jaundice and coagulopathy followed by the development of ascites and/or encephalopathy post hepatic injury is essential for ACLF as per APASL definition [18]. Similar to human ACLF, our animals showed a progressive increase in bilirubin and blood ammonia post APAP/LPS induced liver injury. All animals sacrificed on day 11 showed the presence of ascites with SAAG > 1.1g/dl, hence, conforming to the development of human ACLF. Ballooning degeneration is the precursor of lytic necrosis and has been reported as important histological features in > 50% of ACLF patients [26]. The underlying cause of ballooning degeneration is probably a mitochondrial injury followed by impairment of oxidative phosphorylation, ATP-depletion, loss of energy homeostasis and an increase in permeability of the plasma membrane leading to a ballooning of cells [27]. It reverses if cells repair the loss of damage or may lead to necrosis if the cells fail to restore the energy homeostasis [27]. This raises the possible link between loss of hepatocyte energy and progression of necrosis in response to APAP and LPS in progressive liver injury in ACLF.

Interestingly in the CALPS model, we observed a significant reduction in fibrosis. A reduction in the number of α-SMA + myofibroblasts through apoptosis is a key early event during fibrosis resolution [28]. We observed a significant reduction in α-SMA + myofibroblast post-APAP/LPS treatment. We also observed increased tunnel positive cells in the fibrotic area of the liver; this may be associated with reduction of fibrosis in response to acute injury in the current model. Regression of fibrosis has also been reported in some ACLF patients [18].

The liver has an extraordinary capacity to regenerate on the loss of liver tissue following liver injury due to toxins, surgical resection, infection, or trauma. Compensatory dose dependent increase in liver regeneration with hepatocyte injury has been shown to be associated with spontaneous recovery in various model of drug induced acute live injury [23, 29]. This may be quite different in ACLF. In response to APAP and LPS injury, we observed a progressive reduction in hepatocyte proliferation, even though there was a progressive increase in hepatocyte necrosis. Hence, the loss of compensatory regeneration with progressive hepatocyte death indicates impairment in cellular signaling pathways in chronic liver disease which could be responsible for the rapid progression of liver failure in this model of ACLF. Loss of

hepatocyte replication has also been shown in the human ACLF [24]; however, unlike human ACLF we didn't observed any increased ductular proliferation, an indicator of HPC mediated regeneration. Indeed earlier we have shown that increased HPCs expansion in ACLF does not contribute to outcome and only hepatocyte replication is associated with spontaneous recovery of these patients [24]. Recently, in active infection induced animal model of ACLF, decrease in IL6 and increase in TGF-beta has been shown to be the underlying cause of poor hepatocyte replication. However, we did not find any association of these cytokines with loss of hepatocyte regeneration in our model. In comparison to the cirrhosis, there was a significant increase in hepatic IL-6 within 24 hours post-injury which remained high till day11, while the level of TGF-beta was comparable to that observed in cirrhosis except at 24hrs it decreases (Fig. 2E).

Systemic organ dysfunctions are the common features of ACLF in human [1] of which kidneys are the most affected organs [25]. In the present animal model, while there was little discernible change noticed in the kidney/lung histology between day-0 to 7, at day-11, about 80% of the animals showed features of acute tubular necrosis and 30% of them also showed interstitial and/or exudative pneumonia. This suggests that the kidney damage and renal dysfunction are the consequences and not the precipitant of ACLF. It also shows that the renal dysfunction is due to structural damage of kidney, possibly similar human ACLF [30].

In summary, the CALPS murine model of ACLF shows the clinical and histological features of human ACLF in terms of the presence of jaundice, ascites and acute tubular necrosis and renal dysfunction. It showed that perpetual presence of acute liver injury and endotoxemia trigger hepatocyte ballooning followed by massive hepatocyte necrosis in the presence of chronic liver disease. The acute insult in chronic liver disease triggers regression of fibrosis, concomitant impaired hepatocyte regeneration with on-going liver injury results in liver failure and development of secondary organ injury. This model provides the pathophysiological road-map of the development of ACLF in chronic liver disease in response to acute liver damage and endotoxemia. It is also a representative model for understanding the effects of liver failure on renal injury. This model could help in determining the stage specific interventions to prevent development of portal hypertension, renal and lung injury and also to stimulate hepatic regeneration in the presence of on-going liver injury.

Abbreviations

ACLF, acute-on-chronic liver failure; CCl_4, carbon tetrachloride; APAP, acetaminophen; LPS, lipopolysaccharide; ATN. acute tubular necrosis; SAAG, serum ascites-albumin gradient; SIRS, systemic inflammatory response; TUNEL, Terminal deoxynucleotidyl transferase dUTP nick end labeling.

Declarations

Financial Funding: **T**his work was supported by Science and Engineering Research Board (SERB), Government of India Grant IR/SB/EF/02/2016.

Ethics approval: Animal care and all experimental procedures were approved by the Institutional Animal Ethics Committee (IAEC) under the project approval (IAEC/ILB/17/03) from Department of Science and Technology, Government of India.

Declaration of Conflict of Interest: No authors have any conflict of interest

Author contributions- NN, AK, and SKS contributed to the design of the studies. NN performed the majority of experiments, with assistance from MD, KD, KR and PA. GS and SM help in RT-PCR. SS helped in western blot. CB and RA help in histopathology analysis. AK, RM, SB and SKS assisted with interpretation of the findings. The manuscript was written by NN and AK with critical input from SKS and RM.

Acknowledgement: **T**his work was supported by Science and Engineering Research Board (SERB), Government of India Grant IR/SB/EF/02/2016.

References

1. Sarin SK, Choudhury A. Acute-on-chronic liver failure: terminology, mechanismsand management. Nat Rev Gastroenterol Hepatol. 2016 Mar;13(3):131–49.
2. Arroyo V, Moreau R, Kamath PS, Jalan R, Ginès P, Nevens F, Fernández J, To U, García-Tsao G, Schnabl B. Acute-on-chronic liver failure in cirrhosis. Nat Rev Dis Primers. 2016 Jun;9:2:16041.
3. Bajaj JS, Moreau R, Kamath PS, Vargas HE, Arroyo V, Reddy KR, Szabo G, Tandon P, Olson J, Karvellas C, Gustot T, Lai JC, Wong F. Acute-on-Chronic Liver Failure: Getting Ready for Prime Time? Hepatology. 2018 Oct;68(4):1621–1632.
4. Wu T, Li J, Shao L, Xin J, Jiang L, Zhou Q, Shi D, Jiang J, Sun S, Jin L, Ye P, Yang L, Lu Y, Li T, Huang J, Xu X, Chen J, Hao S, Chen Y, Xin S, Gao Z, Duan Z, Han T, Wang Y, Gan J, Feng T, Pan C, Chen Y, Li H, Huang Y, Xie Q, Lin S, Li L, Li J, Chinese Group on the Study of Severe Hepatitis B (COSSH). Development of diagnostic criteria and a prognostic score for hepatitis B virus-related acute-on-chronic liver failure. Gut. 2018 Dec;67(12):2181–91.
5. Zhao RH, Shi Y, Zhao H, Wu W, Sheng JF. Acute-on-chronic liver failure in chronic hepatitis B: an update. Expert Rev Gastroenterol Hepatol. 2018 Apr;12(4):341–50.
6. Jalan R, Gines P, Olson JC, Mookerjee RP, Moreau R, Garcia-Tsao G, Arroyo V, Kamath PS. Acute-on chronic liver failure. J Hepatol. 2012 Dec;57(6):1336–48.
7. Finkenstedt A, Nachbaur K, Graziadei W, Vogel W. Acute on chronic liver failure: excellent outcomes after liver transplantation but high mortality on the wait list. Liver Transpl. 2013;19:879–86.
8. Kuhla A, Eipel C, Abshagen K, Siebert N, Menger MD, Vollmar B. Role of the perforin/granzyme cell death pathway in D-Gal/LPS-induced inflammatory liver injury. Am J Physiol Gastrointest Liver Physiol. 2009 May;296(5):G1069-76.
9. Li X, Wang LK, Wang LW, Han XQ, Yang F, Gong ZJ. Blockade of high-mobility group box-1 ameliorates acute on chronic liver failure in rats. Inflamm Res. 2013 Jul;62(7):703–9.

10. Balasubramaniyan V, Dhar DK, Warner AE, Vivien Li WY, Amiri AF, Bright B, Mookerjee RP, Davies NA, Becker DL, Jalan R. Importance of Connexin-43 based gap junction in cirrhosis and acute-on-chronic liver failure. J Hepatol. 2013 Jun;58(6):1194–200.
11. Li F, Miao L, Sun H, Zhang Y, Bao X, Zhang D. Establishment of a new acute-on-chronic liver failure model. Acta Pharm Sin B. 2017 May;7(3):326–33.
12. Tripathi DM, Vilaseca M, Lafoz E, Garcia-Calderó H, Viegas Haute G, Fernández-Iglesias A, Rodrigues de Oliveira J, García-Pagán JC, Bosch J, Gracia-Sancho J. Simvastatin Prevents Progression of Acute on Chronic Liver Failure in Rats With Cirrhosis and Portal Hypertension. Gastroenterology. 2018 Nov;155(5):1564–77.
13. Xiang X, Feng D, Hwang S, Ren T, Wang X, Trojnar E, Matyas C, Mo R, Shang D, He Y, Seo W, Shah VH, Pacher P, Xie Q, Gao B. Interleukin-22 ameliorates acute-on-chronic liver failure by reprogramming impaired regeneration pathways in mice. J Hepatol. 2019 Nov 29. pii: S0168-8278(19)30700-7.
14. Fernández J, Acevedo J, Wiest R, Gustot T, Amoros A, Deulofeu C, Reverter E, Martínez J, Saliba F, Jalan R, Welzel T, Pavesi M, Hernández-Tejero M, Ginès P, Arroyo V. European Foundation for the Study of Chronic Liver Failure. Bacterial and fungal infections in acute-on-chronic liver failure: prevalence, characteristics and impact on prognosis. Gut. 2018 Oct;67(10):1870–80.
15. Clària J, Arroyo V, Moreau R. The Acute-on-Chronic Liver Failure Syndrome, or When the Innate Immune System Goes Astray. J Immunol. 2016 Nov 15;197(10):3755–3761.
16. Yang L, Wu T, Li J, Li J. Bacterial Infections in Acute-on-Chronic Liver Failure. Semin Liver Dis. 2018 May;38(2):121–33.
17. Sarin SK, Kedarisetty CK, Abbas Z, Amarapurkar D, Bihari C, Chan AC, Chawla YK, Dokmeci AK, Garg H, Ghazinyan H, Hamid S, Kim DJ, Komolmit P, Lata S, Lee GH, Lesmana LA, Mahtab M, Maiwall R, Moreau R, Ning Q, Pamecha V, Payawal DA, Rastogi A, Rahman S, Rela M, Saraya A, Samuel D, Saraswat V, Shah S, Shiha G, Sharma BC, Sharma MK, Sharma K, Butt AS, Tan SS, Vashishtha C, Wani ZA, Yuen MF, Yokosuka O, APASL ACLF Working Party. Acute-on-chronic liver failure: consensus recommendations of the Asian Pacific Association for the Study of the Liver (APASL) 2014. Hepatol Int. 2014 Oct;8(4):453–71.
18. Sarin SK, Choudhury A, Sharma MK, Maiwall R, Al Mahtab M, Rahman S, Saigal S, Saraf N, Soin AS, Devarbhavi H, Kim DJ, Dhiman RK, Duseja A, Taneja S, Eapen CE, Goel A, Ning Q, Chen T, Ma K, Duan Z, Yu C, Treeprasertsuk S, Hamid SS, Butt AS, Jafri W, Shukla A, Saraswat V, Tan SS, Sood A, Midha V, Goyal O, Ghazinyan H, Arora A, Hu J, Sahu M, Rao PN, Lee GH, Lim SG, Lesmana LA, Lesmana CR, Shah S, Prasad VGM, Payawal DA, Abbas Z, Dokmeci AK, Sollano JD, Carpio G, Shresta A, Lau GK, Fazal Karim M, Shiha G, Gani R, Kalista KF, Yuen MF, Alam S, Khanna R, Sood V, Lal BB, Pamecha V, Jindal A, Rajan V, Arora V, Yokosuka O, Niriella MA, Li H, Qi X, Tanaka A, Mochida S, Chaudhuri DR, Gane E, Win KM, Chen WT, Rela M, Kapoor D, Rastogi A, Kale P, Rastogi A, Sharma CB, Bajpai M, Singh V, Premkumar M, Maharashi S, Olithselvan A, Philips CA, Srivastava A, Yachha SK, Wani ZA, Thapa BR, Saraya A, Shalimar, Kumar A, Wadhawan M, Gupta S, Madan K, Sakhuja P, Vij V, Sharma BC, Garg H, Garg V, Kalal C, Anand L, Vyas T, Mathur RP, Kumar G, Jain P, Pasupuleti SSR, Chawla YK, Chowdhury A, Alam S, Song DS, Yang JM, Yoon EL. APASL ACLF Research Consortium (AARC) for

APASL ACLF working Party. Acute-on-chronic liver failure: consensus recommendations of the Asian Pacific association for the study of the liver (APASL): an update. Hepatol Int. 2019 Jul;13(4):353–390.

19. Choudhury A, Kumar M, Sharma BC, Maiwall R, Pamecha V, Moreau R, Chawla YK, Duseja A, Mahtab M, Rahman S, Hamid SS, Butt AS, Jafri W, Tan SS, Devarbhavi H, Amarapurkar D, Ning Q, Eapen CE, Goel A, Kim DJ, Ghazinyan H, Shiha G, Lee GH, Abbas Z, Payawal DA, Dokmeci AK, Yuen MF, Lesmana LA, Sood A, Chan A, Lau GK, Jia JD, Duan Z, Yu C, Yokosuka O, Jain P, Bhadoria AS, Kumar G, Sarin SK. APASL ACLF working party. Systemic inflammatory response syndrome in acute-on-chronic liver failure: Relevance of 'golden window': A prospective study. J Gastroenterol Hepatol. 2017 Dec;32(12):1989–97.
20. Katoonizadeh A, Laleman W, Verslype C, Wilmer A, Maleux G, Roskams T, Nevens F. Early features of acute-on-chronic alcoholic liver failure: a prospective cohort study. Gut. 2010 Nov;59(11):1561–9.
21. Castellheim A, Brekke OL, Espevik T, Harboe M, Mollnes TE. Innate immune responses to danger signals in systemic inflammatory response syndrome and sepsis. Scand J Immunol. 2009 Jun;69(6):479–91.
22. Cazzaniga M, Dionigi E, Gobbo G, Fioretti A, Monti V, Salerno F. The systemic inflammatory response syndrome in cirrhotic patients: relationship with their in-hospital outcome. J Hepatol. 2009 Sep;51(3):475–82.
23. Bhushan B, Apte U. Liver Regeneration after Acetaminophen Hepatotoxicity: Mechanisms and Therapeutic Opportunities. Am J Pathol. 2019 Apr;189(4):719–29.
24. Shubham S, et al. "Cellular and functional loss of liver endothelial cells correlates with poor hepatocyte regeneration in acute-on-chronic liver failure.". Hepatol Int. 2019;13(6):777–87.
25. Hernaez R, Solà E, Moreau R, Ginès P. Acute-on-chronic liver failure: an update. Gut. 2017 Mar;66(3):541–53.
26. Rastogi A, Maiwall R, Bihari C, Trehanpati N, Pamecha V, Sarin SK. Two-tier regenerative response in liver failure in humans. Virchows Arch. 2014;464:565–73.
27. Chen LY, et al. Promotion of mitochondrial energy metabolism during hepatocyte apoptosis in a rat model of acute liver failure. Mol Med Rep. 2015;12(4):5035–41.
28. Iredale JP, Benyon RC, Pickering J, McCullen M, Northrop M, Pawley S, Hovell C, Arthur MJ. Mechanisms of spontaneous resolution of rat liver fibrosis. Hepatic stellate cell apoptosis and reduced hepatic expression of metalloproteinase inhibitors. J Clin Invest. 1998 Aug 1;102(3):538 – 49.
29. Mehendale HM. Tissue repair: an important determinant of final outcome of toxicant-induced injury. Toxicol Pathol. 2005;33(1):41–51.
30. Maiwall R, et al. "AKI in patients with acute on chronic liver failure is different from acute decompensation of cirrhosis. " Hepatol Int. 2015;9(4):627–39.

Figures

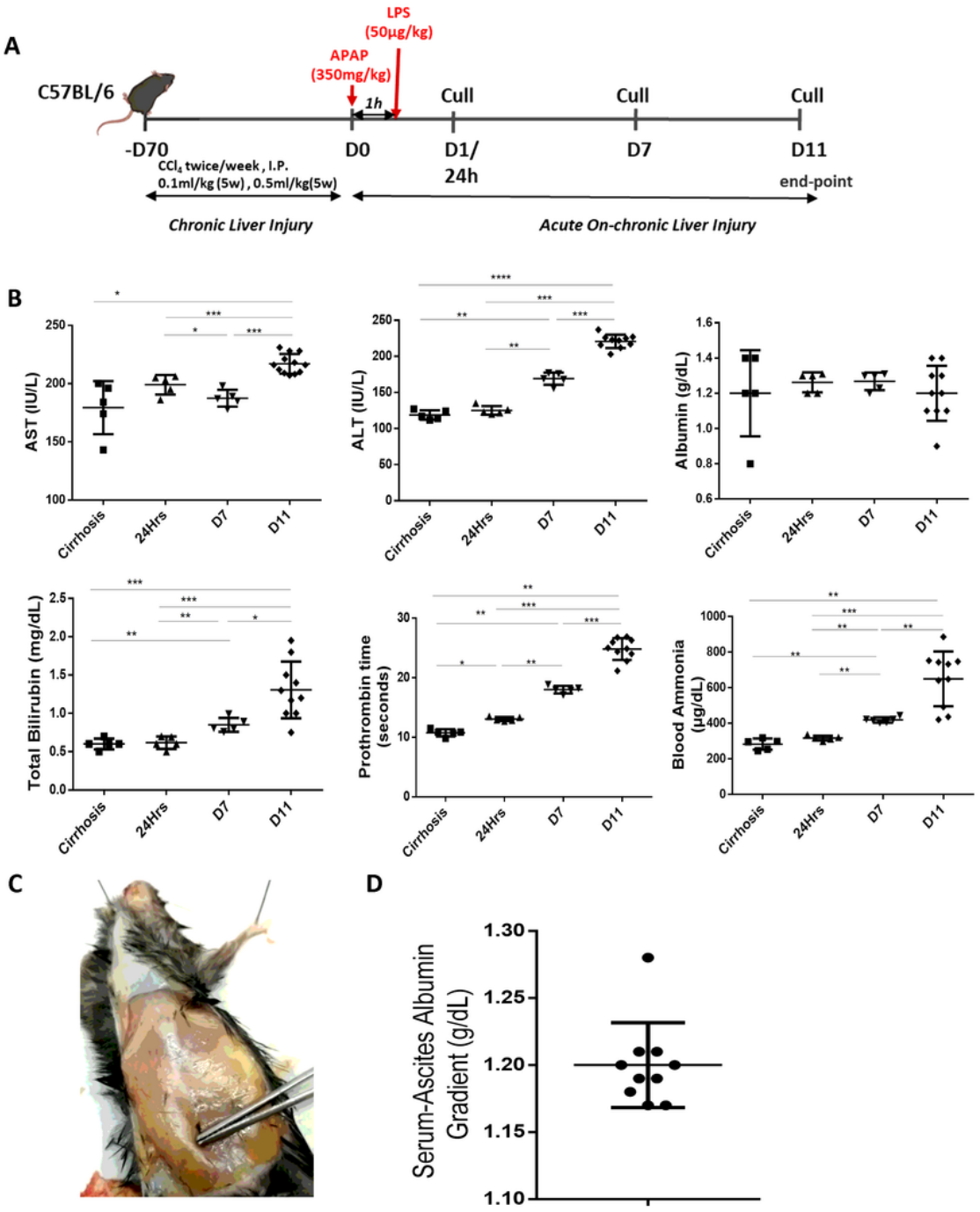

Figure 1

Development of ACLF mice model. (A) Representative diagram of ACLF induction and time points of investigation. (B) Bar-graph showing blood biochemical analysis of mice sacrificed at 24hrs, day-7 and day-11 of analysis in comparison to cirrhosis. (C) Representative image showing the mice sacrificed at day 11 shows the abdominal bulging with the presence of jaundice and ascitic fluid. (D) Bar-graph

showing the measured SAAG value (>1g/dL SAAG is an indicator of ascites development due to liver failure); p=*<0.05; p=**<0.005; p=***<0.0005; p=****<0.0001.

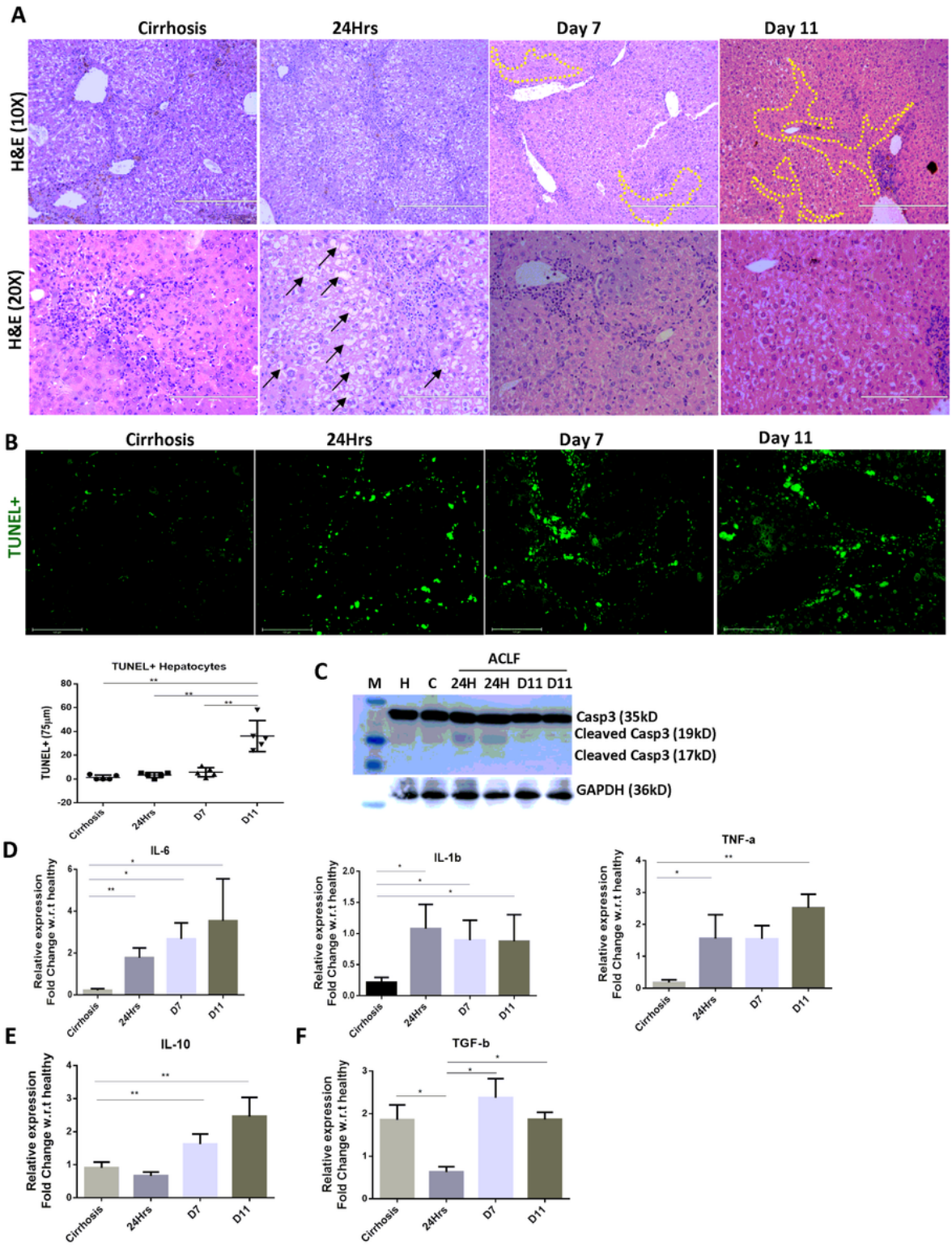

Figure 2

Immunohistochemical and quantitative analysis for progressive liver injury and inflammation. (A) Representative micrograph showing H&E staining of ACLF and cirrhotic mice (magnification 10X and 20X; yellow dashed lines marking necrotic area; arrows marking hepatocytes ballooning). (B)

Representative micrograph and bar graph showing TUNEL positive cells of ACLF and cirrhotic liver tissue (magnification 10X; N=5 in each group). (C) Representative micrograph showing the protein expression of Caspase-3. (D) Bar graph showing the relative mRNA level of pro-inflammatory cytokines of ACLF group and cirrhosis. (E) Bar- graph showing the relative mRNA level of anti-inflammatory cytokines of ACLF group and cirrhosis. (F) Bar- graph showing the relative mRNA level of TGF-β. M=marker, H=healthy, C=cirrhosis, 24H=ACLF 24hours, D11=ACLF Day 11; p= *<0.05; **<0.005; N=5 in each group.

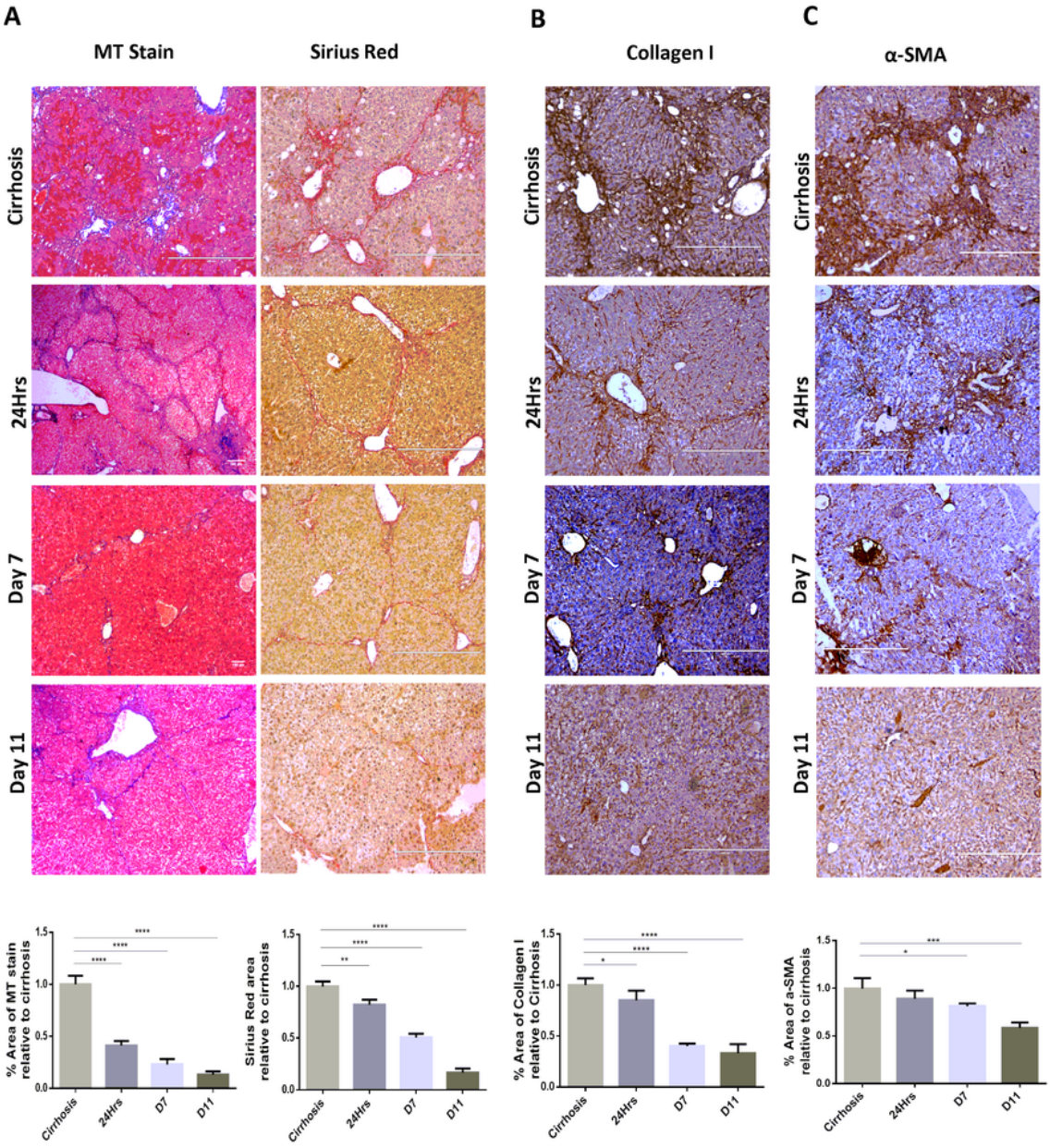

Figure 3

Immunohistochemical analysis for fibrosis status in cirrhotic and ACLF liver. (A) Representative micrograph showing fibrosis staining through MT and sirius red (magnification 4X), bar-diagram showing % of MT and sirius red stained septa relative to cirrhosis. (B) Representative micrograph showing IHC staining of collagen I (magnification 4X), bar-diagram showing % of collagen I in ACLF relative to cirrhosis. (C) Representative micrograph showing IHC staining of α-SMA (magnification 4X), bar-diagram showing % of α-SMA+ myofibrobast cells in ACLF relative to cirrhosis. p= *<0.05; **<0.005; ***<0.0005; ****<0.0001, N=5 in each group.

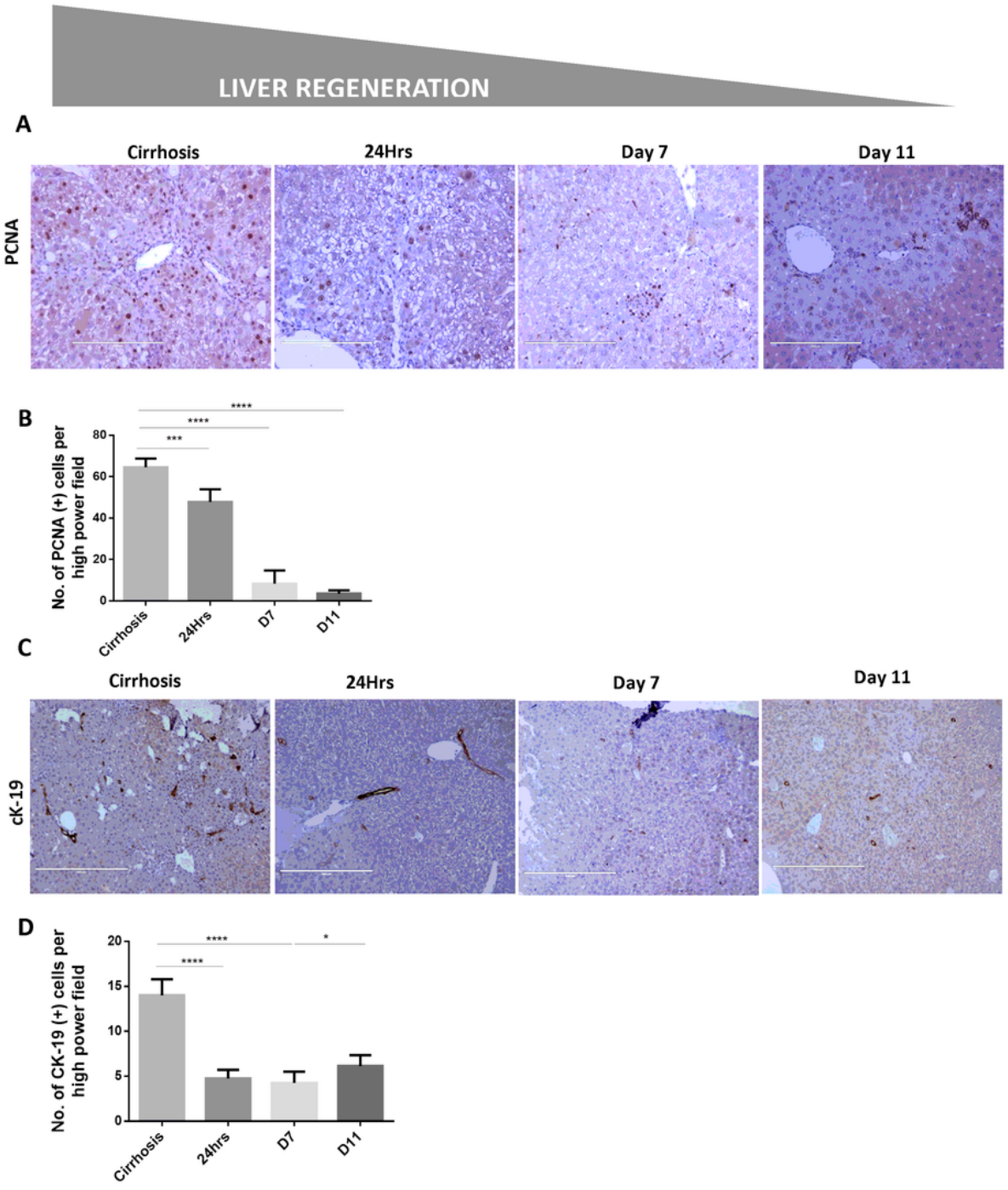

Figure 4

Immunohistochemical analysis for regeneration status in ACLF mice. (A) Representative micrograph showing IHC staining of PCNA hepatocytes in ACLF and cirrhotic liver tissue (magnification 20X). (B) Representative micrograph showing IHC staining for cK-19 in ACLF and cirrhotic liver tissue (magnification 20X). (C) Quantitative analysis of PCNA positive hepatocytes per high power field. (D) Quantitative analysis of ck-19 positive cells per high power field. p= *<0.05; **<0.005; ****<0.0001, N=5 in each group.

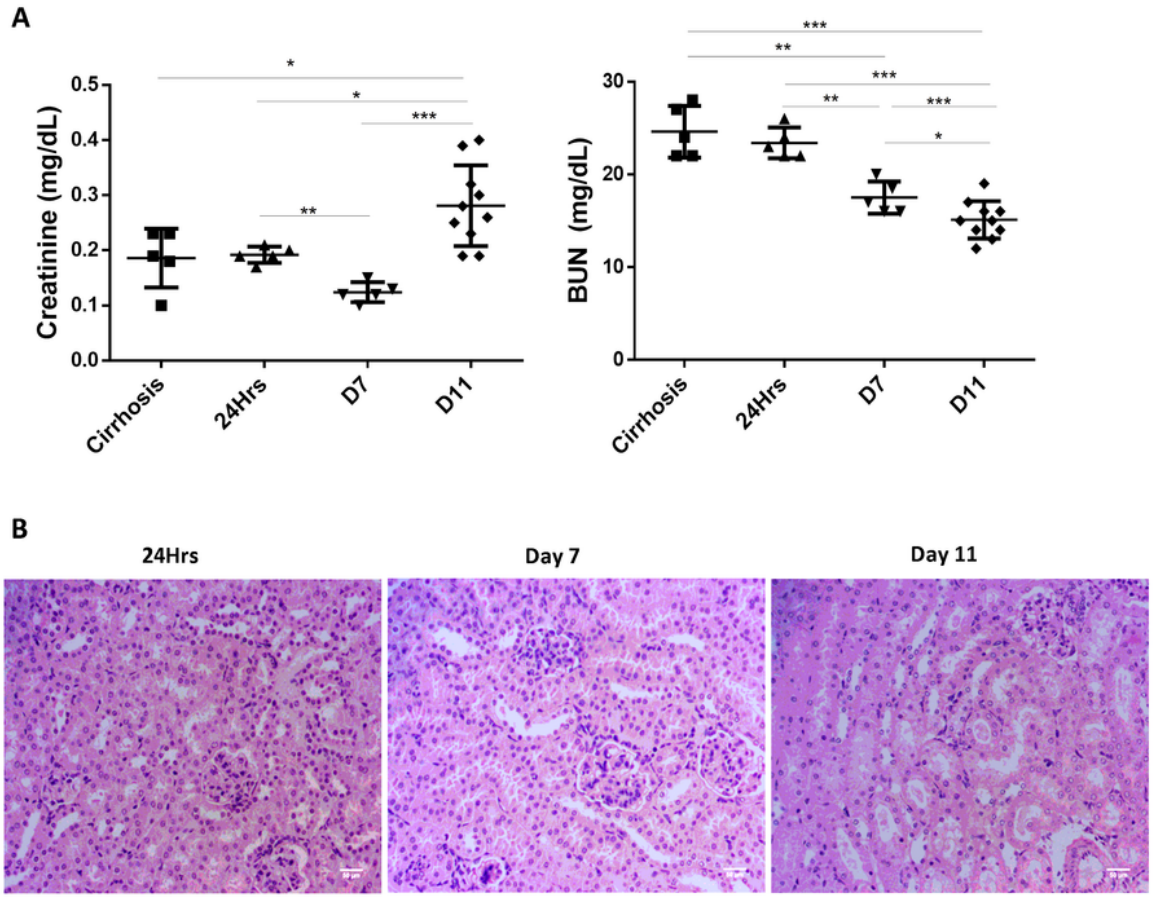

Figure 5

Systemic organ dysfunctions in ACLF. (A) Bar-graph showing the blood biochemical level of creatinine (mg/dL) and BUN (mg/dL) in ACLF and Cirrhosis. (B) Representative micrographs showing the hematoxylin and eosin stained kidney sections of ACLF groups at different time points (magnification 10X). p= *<0.05; **<0.005; ***<0.0005.

Supplementary Files

This is a list of supplementary files associated with this preprint. Click to download.

- Onlinefloatimage1.png
- Supplementarydata13042021.docx